Electronic Supplementary Material (ESI) for Soft Matter.
This journal is © The Royal Society of Chemistry 2017

# Electronic Supplementary Information for:

# Macromolecular ‘size’ and ‘hardness’ drives structure in solvent-swollen blends of linear, cyclic, and star polymers

Thomas E. Gartner, III;[1] Arthi Jayaraman[1,2,*]

[1]Department of Chemical and Biomolecular Engineering, 150 Academy Street, Colburn Laboratory, University of Delaware, Newark, DE 19716

[2]Department of Materials Science and Engineering, University of Delaware, Newark, DE 19716

*Corresponding author arthij@udel.edu

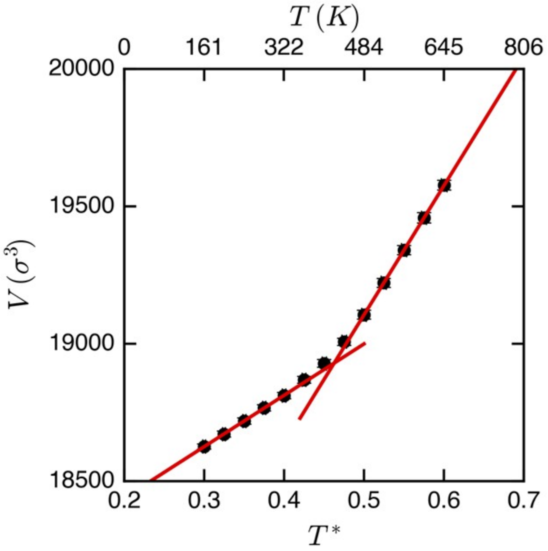

**Figure S1:** Simulation box volume (*V*) as a function of temperature (*T**) for a neat polystyrene (PS) melt, with model details as described in the main text methods section. Black squares are the results of three independent NPT simulation trials at each temperature and atmospheric pressure ($P^* = 0.0086$). Each trial was started from an equilibrated initial configuration that was prepared at $T^* = 1.0$, followed by 5 x $10^6$ timesteps of equilibration and 5 x $10^6$ timesteps of sampling at the desired temperature. Red lines are fits to the 5 highest and 5 lowest temperatures, respectively, and we define the glass transition temperature ($T_g$) to be the intersection of the two lines, at $T^* = 0.463$. We investigated multiple other simulation and $T_g$ calculation protocols,[1-3] including sequential and continuous decreases in temperature as well as fits to differing numbers of data points, which provided equivalent results to the method reported here.

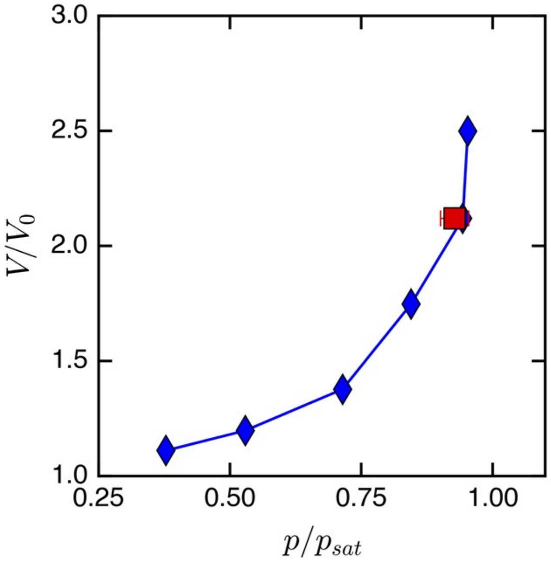

**Figure S2:** Degree of swelling of the polymer phase (*V*/*V*$_0$) as a function of annealing vapor composition ($p/p_{sat}$) for a system size of fifty 21mer linear chains, 500 nitrogen beads, and 730 to 8,230 solvent beads (blue diamonds), and a larger system size of five hundred 21mer linear chains, 5,000 nitrogen beads, and 62,300 solvent beads (red square). The two system sizes produced equivalent swelling results.

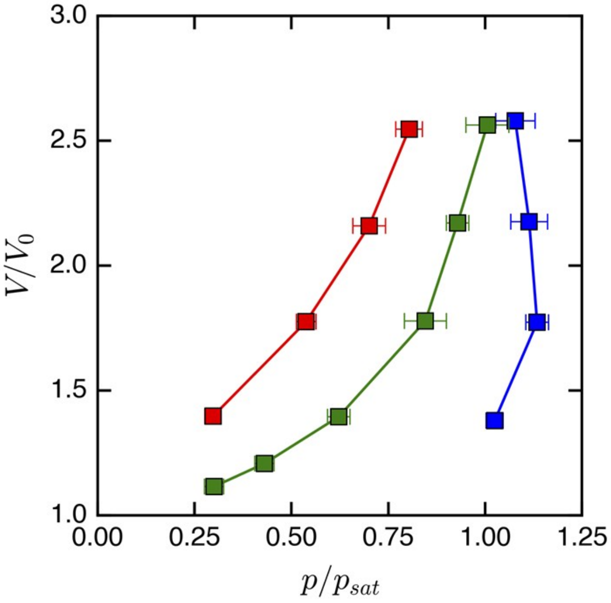

**Figure S3:** Degree of swelling of the polymer phase ($V/V_0$) as a function of annealing vapor composition ($p/p_{sat}$) for linear 21mer chains with polymer-solvent nonbonded Lennard-Jones energy parameter $\varepsilon_{PS} = 0.60$ (red squares), $\varepsilon_{PS} = 0.66$ (green squares), and $\varepsilon_{PS} = 0.74$ (blue squares). The strength of the polymer-solvent attraction tunes the location and slope of the $V/V_0$ curve, which allows this model to be adjusted to another polymer-solvent system of interest, provided that experimental swelling data is available.

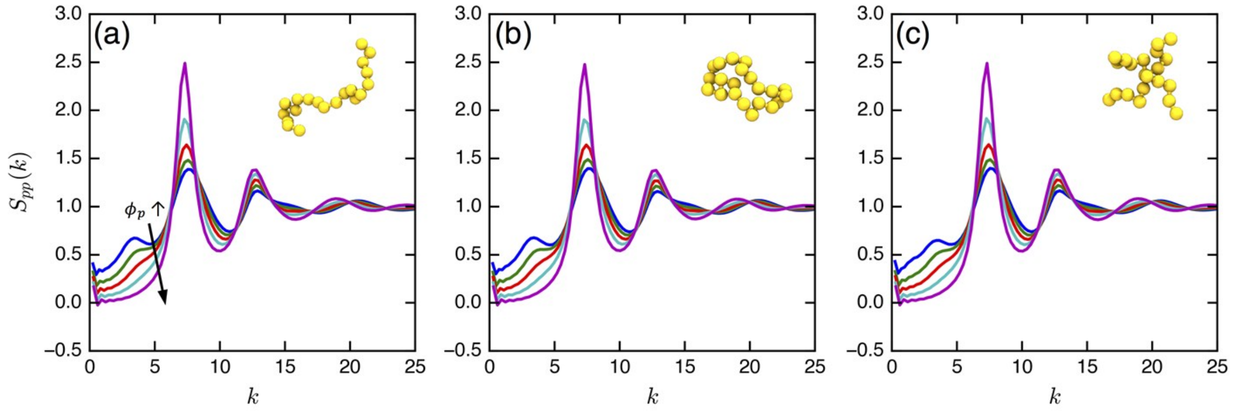

**Figure S4:** Polymer-polymer structure factor, $S_{pp}(k)$, for (a) linear, (b) cyclic, and (c) 4-arm star polystyrene chains in toluene. Colors denote the polymer volume fraction, $\phi_p$, with blue, green, red, cyan, and magenta representing $\phi_p$ = 0.5, 0.6, 0.7, 0.8, and 0.9 respectively. The black arrow in (a) indicates the direction of increasing $\phi_p$. We observe minimal differences between the $S_{pp}(k)$ for different polymer architectures at a given solvent content, but stronger polymer-polymer correlations as the solvent content decreases.

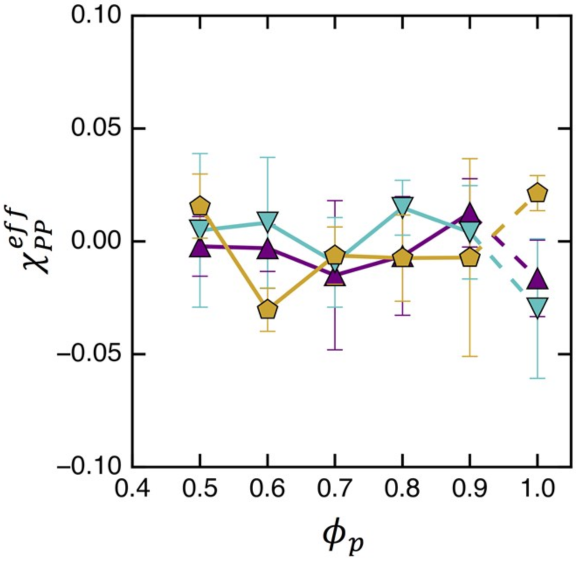

**Figure S5:** PRISM polymer-polymer effective interaction parameter, $\chi_{PP}{}^{eff}$, as a function of $\phi_p$ for equimolar linear-cyclic (purple upward facing triangles), linear-star (cyan downward facing triangles), and cyclic-star (gold pentagons) blends. The dotted lines between $\phi_p = 0.9$ and $\phi_p = 1.0$ are to denote that the $\phi_p = 1.0$ condition is at $T^* = 0.556$. Within the resolution of our PRISM $\chi_{PP}{}^{eff}$ analysis, there are minimal differences in the polymer-polymer effective interactions as a function of chain architecture or solvent content.

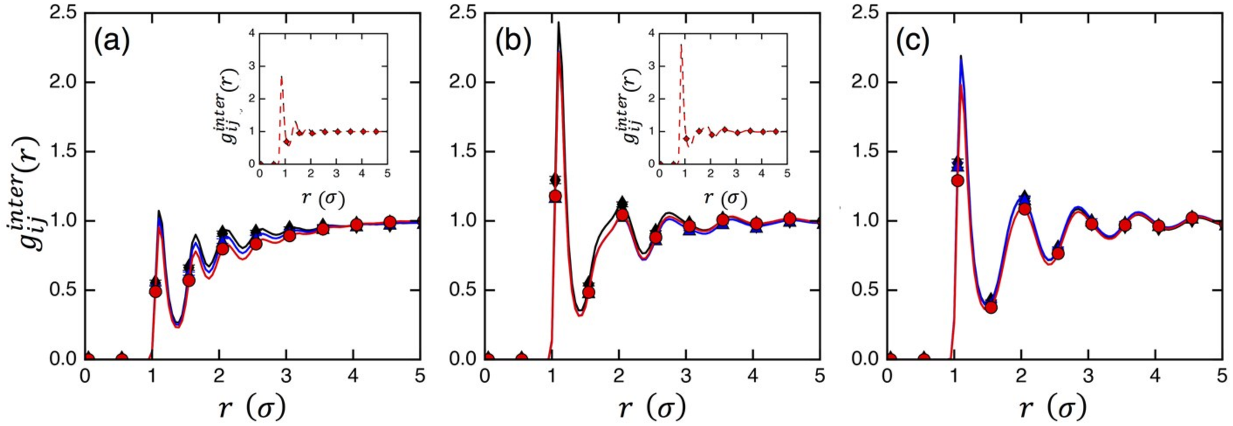

**Figure S6:** Intermolecular bead-bead $g(r)$ in a linear-star blend at (a) $\phi_p = 0.5$, (b) $\phi_p = 0.9$, and (c) $\phi_p = 1.0$, $T^* = 0.556$. Linear bead-linear bead pairs are plotted with black diamonds, linear bead-star bead pairs are plotted with blue upward facing triangles, and star bead-star bead pairs are plotted with red circles. Black and red dotted lines in the inset plots in (a,b) are linear bead-solvent and star bead-solvent pairs, respectively. Similar to the linear-cyclic system presented in the main text, linear-linear correlations are strongest, followed by linear-star and star-star, which we attribute to the 'softness' of the linear chains allowing other molecules to approach more closely. Solvent-polymer correlations are identical between linear and star chains.

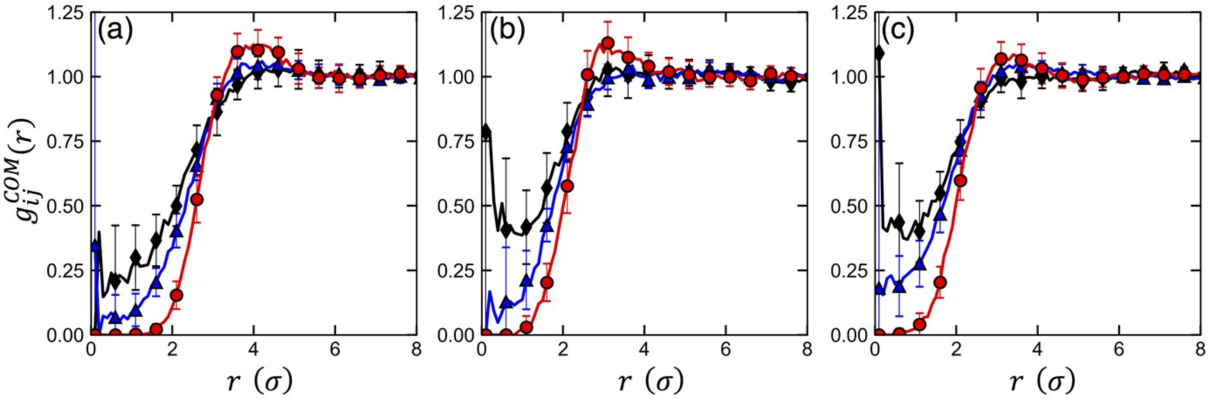

**Figure S7:** Radial distribution function between chain center-of-mass ($g^{COM}(r)$) for the linear-star blend system. Polymer volume fractions displayed are (a) $\phi_p = 0.5$, (b) $\phi_p = 0.9$, and (c) $\phi_p = 1.0$, $T^* = 0.556$. Linear chain-linear chain pairs are plotted with black diamonds, linear chain-star chain pairs are plotted with blue triangles, and star chain-star chain pairs are plotted with red circles. As in the linear-cyclic system discussed in the main text, the star chain-star chain $g^{COM}(r)$ shows preferential star-star packing at intermediate distances, while the linear chain-linear chain $g^{COM}(r)$ smoothly increases to the bulk value.

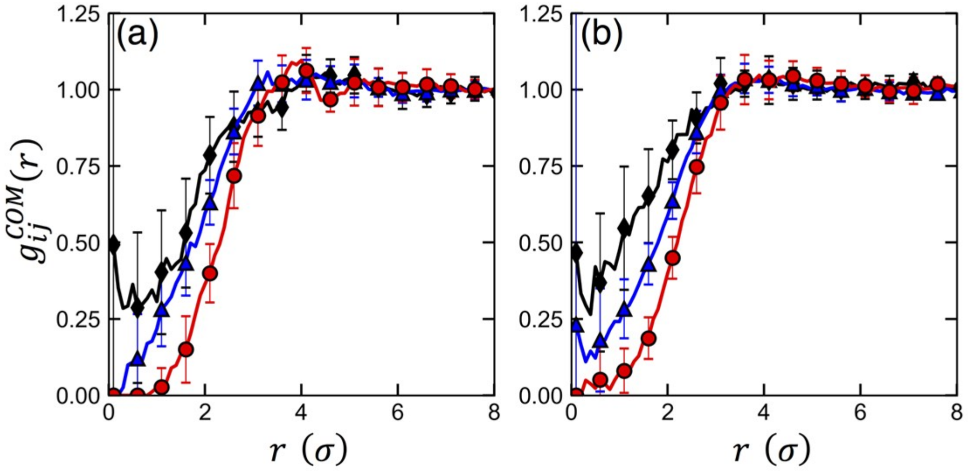

**Figure S8:** Radial distribution function between chain center-of-mass ($g^{COM}(r)$) for a blend of 21mer linear chains and 33mer 4-arm star chains. These molecular weights were chosen to approximately match the radius of gyration between the linear and star chains, for example, at $\phi_p = 0.9$, $R_{g,linear} \approx 2.21\ \sigma$ and $R_{g,star} \approx 2.30\ \sigma$. Polymer volume fractions displayed are (a) $\phi_p = 0.9$, and (b) $\phi_p = 1.0$, $T^* = 0.556$. Linear chain-linear chain pairs are plotted with black diamonds, linear chain-33mer star chain pairs are plotted with blue triangles, and 33mer star chain-33mer star chain pairs are plotted with red circles. In contrast to the behavior seen in Supplementary Information Figure S7 above, both the linear chain-linear chain and 33mer star chain-33mer star chains exhibit a mild peak in the $g^{COM}(r)$ at intermediate distances, qualitatively matching the results from the soft-sphere simulations in which the spheres are approximately the same size (main text Figure 7).

## References:

1. W. L. Merling, J. B. Mileski, J. F. Douglas and D. S. Simmons, *Macromolecules*, 2016, **49**, 7597-7604.
2. A. Chremos and J. F. Douglas, *J. Chem. Phys.*, 2015, **143**, 111104.
3. P. N. Patrone, A. Dienstfrey, A. R. Browning, S. Tucker and S. Christensen, *Polymer*, 2016, **87**, 246-259.